ARTICLE
Journal of Cellular Biochemistry 114:2293–2305 (2013)

Journal of Cellular Biochemistry

# Metabolic Stability of 3-Epi-1α,25-Dihydroxyvitamin $D_3$ Over 1α,25-Dihydroxyvitamin $D_3$: Metabolism and Molecular Docking Studies Using Rat CYP24A1

Steve Y. Rhieu,[1,2,3] Andrew J. Annalora,[4] Guochun Wang,[1,2,3] Caroline C. Flarakos,[5] Rose M. Gathungu,[5] Paul Vouros,[5] Rita Sigüeiro,[6] Antonio Mouriño,[6] Inge Schuster,[7] G. Tayhas R. Palmore,[2,3,8] and G. Satyanarayana Reddy[1]*

[1]*Epimer LLC, North Smithfield, Rhode Island, 02896*
[2]*Division of Biology and Medicine, Brown University, Providence, Rhode Island, 02912*
[3]*School of Engineering, Brown University, Providence, Rhode Island, 02912*
[4]*Department of Molecular Biology, The Scripps Research Institute, La Jolla, California, 92037*
[5]*Department of Chemistry and Chemical Biology, Northeastern University, Boston, Massachusetts, 02115*
[6]*Departamento de Química Orgánica, Laboratorio de Investigación Ignacio Ribas, Universidad de Santiago de Compostela, E-15706, Santiago de Compostela, Spain*
[7]*Institute for Theoretical Chemistry, University of Vienna, Vienna, Austria*
[8]*Department of Chemistry, Brown University, Providence, Rhode Island, 02912*

## ABSTRACT

3-epi-1α,25-dihydroxyvitamin $D_3$ (3-epi-1α,25$(OH)_2D_3$), a natural metabolite of 1α,25-dihydroxyvitamin $D_3$ (1α,25$(OH)_2D_3$), exhibits potent vitamin D receptor (VDR)-mediated actions such as inhibition of keratinocyte growth or suppression of parathyroid hormone secretion. These VDR-mediated actions of 3-epi-1α,25$(OH)_2D_3$ needed an explanation as 3-epi-1α,25$(OH)_2D_3$, unlike 1α,25$(OH)_2D_3$, exhibits low affinity towards VDR. Metabolic stability of 3-epi-1α,25$(OH)_2D_3$ over 1α,25$(OH)_2D_3$ has been hypothesized as a possible explanation. To provide further support for this hypothesis, we now performed comparative metabolism studies between 3-epi-1α,25$(OH)_2D_3$ and 1α,25$(OH)_2D_3$ using both the technique of isolated rat kidney perfusion and purified rat CYP24A1 in a cell-free reconstituted system. For the first time, these studies resulted in the isolation and identification of 3-epi-calcitroic acid as the final inactive metabolite of 3-epi-1α,25$(OH)_2D_3$ produced by rat CYP24A1. Furthermore, under identical experimental conditions, it was noted that the amount of 3-epi-calcitroic acid produced from 3-epi-1α,25$(OH)_2D_3$ is threefold less than that of calcitroic acid, the analogous final inactive metabolite produced from 1α,25$(OH)_2D_3$. This key observation finally led us to conclude that the rate of overall side-chain oxidation of 3-epi-1α,25$(OH)_2D_3$ by rat CYP24A1 leading to its final inactivation is slower than that of 1α,25$(OH)_2D_3$. To elucidate the mechanism responsible for this important finding, we performed a molecular docking analysis using the crystal structure of rat CYP24A1. Docking results suggest that 3-epi-1α,25$(OH)_2D_3$, unlike 1α,25$(OH)_2D_3$, binds to CYP24A1 in an alternate configuration that destabilizes the formation of the enzyme-substrate complex sufficiently

Steve Y. Rhieu and Andrew J. Annalora contributed equally to this work.
Conflict of interest: The authors have no conflict of interest to declare.

Grant sponsor: National Institutes of Health; Grant number: DK52488; Grant sponsor: Epimer LLC; Grant sponsor: Teijin Pharma Ltd.; Grant sponsor: The National Cancer Institute; Grant number: 1R01CA69390; Grant sponsor: Spanish MCI; Grant number: SAF2010-15291; Grant sponsor: National Science Foundation GK-12 Teaching Fellowship; Grant sponsor: The Scripps Research Institute.

Steve Y. Rhieu's present address is National Institute of Standards and Technology, Gaithersburg, Maryland, 20899.
*Correspondence to: Dr. G. Satyanarayana Reddy, M.D., Epimer LLC, 1 Valley View Drive, North Smithfield, RI 02896.
E-mail: satyareddy125@gmail.com

Manuscript Received: 18 March 2013; Manuscript Accepted: 12 April 2013
Accepted manuscript online in Wiley Online Library (wileyonlinelibrary.com): 20 April 2013
DOI 10.1002/jcb.24576 • © 2013 Wiley Periodicals, Inc.

to slow the rate at which 3-epi-1α,25(OH)$_2$D$_3$ is inactivated by CYP24A1 through its metabolism into 3-epi-calcitroic acid. J. Cell. Biochem. 114: 2293–2305, 2013. 

**KEY WORDS:** 3-EPI-1α,25-DIHYDROXYVITAMIN D$_3$; 3-EPI-CALCITROIC ACID; C-3 EPIMERIZATION PATHWAY; 3-EPI-VITAMIN D$_3$; CYP24A1; MOLECULAR DOCKING

The secosteroid hormone, 1α,25-dihydroxyvitamin D$_3$ (1α,25(OH)$_2$D$_3$), is the natural ligand for the vitamin D receptor (VDR), a member of the nuclear receptor superfamily [Brumbaugh and Haussler, 1975]. In response to hormone binding, the VDR regulates the transcription of a wide array of genes, which encodes osteocalcin, calbindin, and many other proteins involved in various pathophysiological systems [Bouillon et al., 1995; Plum and DeLuca, 2010; Verstuyf et al., 2010]. The VDR bound to 1α,25(OH)$_2$D$_3$ also induces expression of mitochondrial cytochrome P450 24A1 (CYP24A1), a multicatalytic enzyme that sequentially oxidizes the side-chain of 1α,25(OH)$_2$D$_3$, leading to loss of its hormonal activity [Akiyoshi-shibata et al., 1994; Sakaki et al., 1999; Schuster, 2011]. The metabolic inactivation of 1α,25(OH)$_2$D$_3$ by CYP24A1 proceeds mainly through the C-24 oxidation pathway, resulting in its conversion into a side-chain cleaved inactive water-soluble metabolite, calcitroic acid [Esvelt et al., 1979; Makin et al., 1989; Reddy and Tserng, 1989].

Aside from the above mentioned C-24 oxidation pathway, 1α,25(OH)$_2$D$_3$ is also metabolized through the C-3 epimerization pathway [Reddy et al., 1994, 2000, 2001; Bischof et al., 1998; Sekimoto et al., 1999; Siu-Caldera et al., 1999a; Astecker et al., 2000; Masuda et al., 2000], leading to the formation of 3-epi-1α,25-dihydroxyvitamin D$_3$ (3-epi-1α,25(OH)$_2$D$_3$) as a result of change in the configuration of C-3 hydroxyl group in the A-ring from β to α (Fig. 1). The C-3 epimerization pathway is tissue specific as 3-epi-1α,25(OH)$_2$D$_3$ is produced only in specific tissues [Reddy et al., 1997, 2001; Siu-Caldera et al., 1999a; Masuda et al., 2000]. More interestingly, 3-epi-1α,25(OH)$_2$D$_3$ exerts significant biological activities in the tissues in which it is produced. As such, 3-epi-1α,25(OH)$_2$D$_3$ was found to be almost equipotent to 1α,25(OH)$_2$D$_3$ in inhibiting the growth of human keratinocytes [Norman et al., 1993; Schuster et al., 1997; Molnár et al., 2011], suppressing parathyroid hormone secretion in bovine parathyroid cells [Brown et al., 1999], stimulating surfactant synthesis in human alveolar type II cells [Rehan et al., 2002], and increasing alveolar septal thinning during perinatal lung maturation in the rat [Sakurai et al., 2009]. In light of prospective clinical applications, the biological activities of 3-epi-1α,25(OH)$_2$D$_3$ observed in both in vitro and in vivo studies in conjunction with its low calcemic activity [Norman et al., 1993; Fleet et al., 1996] make it a promising therapeutic agent.

To date, the underlying mechanisms for the apparent VDR-mediated biological activities of 3-epi-1α,25(OH)$_2$D$_3$, however, remain unexplained because of its low binding affinity for the VDR [Norman et al., 1993; Brown et al., 1999; Harant et al., 2000]. The metabolic stability of 3-epi-1α,25(OH)$_2$D$_3$ has been speculated as one possible mechanism [Brown et al., 1999; Astecker et al., 2000] that may potentially prolong the duration of the VDR-mediated gene expression by 3-epi-1α,25(OH)$_2$D$_3$. However, a definite evidence for this speculation has not been established yet. Therefore, we undertook the present study. We compared the metabolism of 3-epi-1α,25(OH)$_2$D$_3$ with that of its parent compound 1α,25(OH)$_2$D$_3$ using both the technique of isolated rat kidney perfusion and purified rat CYP24A1 in a cell-free reconstituted system. These studies finally led to the isolation and identification of 3-epi-calcitroic acid, a water-soluble end product of 3-epi-1α,25(OH)$_2$D$_3$ metabolism by rat CYP24A1. It was noted that the amount of 3-epi-calcitroic acid

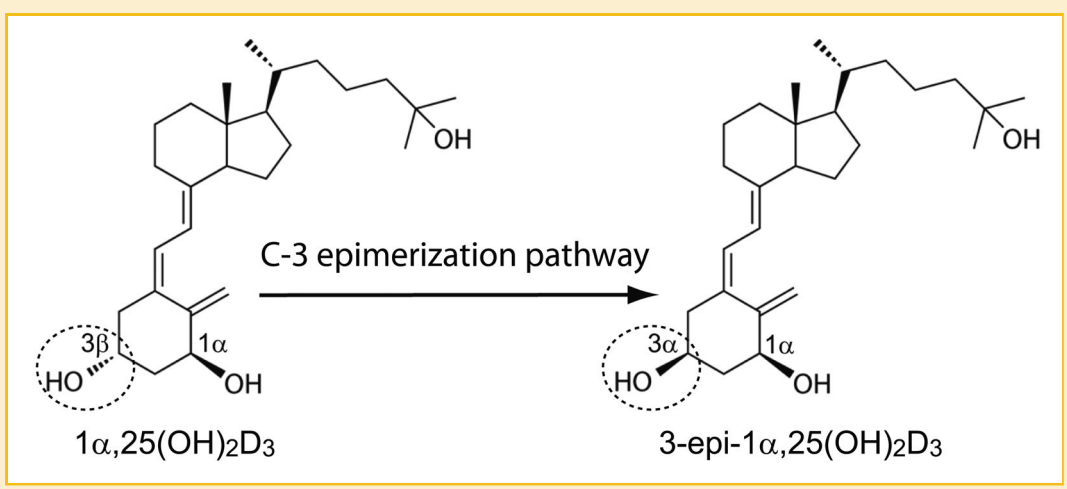


**Fig. 1.** Metabolism of 1α,25(OH)$_2$D$_3$ into 3-epi-1α,25(OH)$_2$D$_3$ through the C-3 epimerization pathway.

produced from 3-epi-1α,25(OH)$_2$D$_3$ was threefold lower than that of calcitroic acid produced from 1α,25(OH)$_2$D$_3$ under identical conditions. This finding finally provided unequivocal experimental proof to show that the rate of side-chain oxidation of 3-epi-1α,25(OH)$_2$D$_3$ is slower than that of 1α,25(OH)$_2$D$_3$. To gain an insight into the structural determinants of substrate recognition, a molecular docking analysis was carried out using the crystal structure of rat CYP24A1 as a means to understand the reason for the metabolic stability of 3-epi-1α,25(OH)$_2$D$_3$ over 1α,25(OH)$_2$D$_3$.

## MATERIALS AND METHODS

### VITAMIN D COMPOUNDS AND CHEMICALS

Crystalline 25-hydroxyvitamin-D$_3$ (25(OH)D$_3$) and 1α,25(OH)$_2$D$_3$ were a gift from Dr. Milan R. Uskokovic from Hofmann-La Roche, Inc. 3-epi-1α,25(OH)$_2$D$_3$ was synthesized according to a published method [Molnár et al., 2011]. Cholacalcioic acid was synthesized as previously described [Reddy et al., 2006]. All other chemicals were purchased from Sigma-Aldrich (St. Louis, MO).

### TECHNIQUE OF ISOLATED RAT KIDNEY PERFUSION

The technique of isolated rat kidney perfusion was performed as described previously [Reddy et al., 1982a, 1983, 1987]. This study was approved by the animal care committee at Women and Infants Hospital of Rhode Island (Providence, RI). Male Sprague-Dawley rats (350–375 g) were pre-treated intraperitoneally with 2 μg of 1α,25(OH)$_2$D$_3$ to increase the activity of CYP24A1 prior to surgical excision of the kidney and the perfusions were performed at a substrate concentration of 1 μM. Each kidney was perfused with 50 ml of perfusate containing 20.8 μg of either 3-epi-1α,25(OH)$_2$D$_3$ or 1α,25(OH)$_2$D$_3$ for a period of 2 h. Three separate kidney perfusions were performed for each compound.

### CYP24A1 RECONSTITUTION ASSAY

Recombinant rat CYP24A1 (WT, Δ2-32) was expressed in *Escherichia coli* (DH5α-FIQ) and purified as described [Annalora et al., 2004]. Purified CYP24A1 samples with $A_{417}/A_{280}$ ratio exceeding 1.0 were considered pure for biochemical assay. Bovine adrenodoxin (ADX) and adrenodoxin reductase (ADR) were expressed and purified as described with minor modifications [Gnanaiah and Omdahl, 1986; Sagara et al., 1993]. Spectral purity indexes of ADX ($A_{414}/A_{276}$) and ADR ($A_{452}/A_{278}$) used in the present study were 0.9 and 0.1, respectively [Kimura et al., 1978; Annalora et al., 2004]. All enzymes were stored at −80°C prior to use. The reconstituted CYP24A1 reaction mixture (1 ml) contained 50 mM phosphate buffer (pH 7.4), CYP24A1 (0.5 μM), ADX (0.5 μM), ADR (0.5 μM), and vitamin D compounds at different concentrations (1–5 μM). The reaction was initiated by the addition of NADPH at a final concentration of 1 mM and the mixture was incubated at 37°C for 5–60 min. The reaction was stopped with 2 ml of methanol.

### HIGH PERFORMANCE LIQUID CHROMATOGRAPHY (HPLC)

HPLC analysis of the lipid extracts of perfusate samples from kidney perfusions or the incubation mixtures from CYP24A1 reconstitution assay were performed with a Waters System Controller (Waters, Milford, MA). A photodiode array detector (Waters model 996) was used to monitor lipids with the typical vitamin D chromophore ($\lambda_{max}$ at 265 nm; $\lambda_{min}$ at 228 nm). Both lipid- and water-soluble metabolites were analyzed by different HPLC systems as described below.

### EXTRACTION OF LIPID-SOLUBLE METABOLITES PRODUCED BY THE RAT KIDNEY AND THEIR ANALYSIS BY HPLC

The final 50 ml of perfusate at the end of each kidney perfusion was collected and subjected to lipid extraction using the method described before [Reddy and Tserng, 1989]. Prior to lipid extraction, 25(OH)D$_3$ was added to each sample as an internal standard to quantify the efficiency of the lipid extraction procedure. The total dried lipid extract of perfusate was dissolved in 500 μl of 15% isopropanol in hexane and was analyzed by a straight phase HPLC system using a Zorbax-SIL column (250 mm × 4.6 mm) (Dupont, Wilmington, DE) eluted with 15% isopropanol in hexane at a flow rate of 2 ml/min. Each peak from the first HPLC system was further purified by a second straight phase HPLC system using the same Zorbax-SIL column eluted with 10% isopropanol in methylene chloride at a flow rate of 2 ml/min.

### EXTRACTION OF BOTH LIPID AND WATER-SOLUBLE METABOLITES PRODUCED BY CYP24A1 AND THEIR ANALYSIS BY HPLC

Each final 1 ml of the incubation mixture from CYP24A1 reconstitution assay was quenched with 2 ml of methanol. Prior to the extraction procedure, we added 25(OH)D$_3$ and cholacalcioic acid to each incubation mixture as internal standards to quantify the efficiency of the extraction of both lipid- and water-soluble metabolites, respectively. Then 4 ml of dichloromethane was added and mixed thoroughly. This resulted in the separation of the dichloromethane fraction from the methanol/water fraction. The dichloromethane fraction was collected and evaporated under a stream of nitrogen. The residue was dissolved in 500 μl of 15% isopropanol in hexane for HPLC analysis. We then proceeded to re-extract the aqueous layer which was first acidified with a drop of hydrochloric acid (concentrated) followed by the addition of 4 ml of dichloromethane and the above procedure was repeated. The first extract (extract #1), containing the unmetabolized substrate and all the less polar lipid-soluble metabolites along with the internal standard 25(OH)D$_3$ was analyzed by a straight phase HPLC system using a Zorbax-SIL column (250 mm × 4.6 mm) (Dupont, Wilmington, DE) eluted with 15% isopropanol in hexane at a flow rate of 2 ml/min. The second extract (extract #2) containing the highly polar water-soluble-metabolite(s) along with the internal standard cholacalcioic acid was analyzed by a straight phase HPLC system using the same Zorbax-SIL column as above eluted with 10% isopropanol and 10% methanol in hexane at a flow rate of 2 ml/min.

### GAS CHROMATOGRAPHY-MASS SPECTROMETRY (GC-MS)

GC-MS analysis was performed using an Agilent GC system 6890 equipped with a mass-selective detector (MSD5973). Purified metabolites were subjected to trimethylsilyl (TMS) derivatization using Power SIL-Prep (Alltech Associates, Deerfield, IL) in anhydrous acetonitrile (50:50, v/v) at 70°C for 15 min. The derivatized metabolites (final concentration, 1 μg/ml) were subjected to GC-MS analysis using a HP-5MS GC capillary column (30 m × 0.25 mm

$\times$ 0.25 μm, 5% phenyl siloxane) with helium as a carrier gas at a flow rate of 0.8 ml/min. The oven temperature was set at 150°C and ramped at a rate of 10°C/min to reach the final temperature of 300°C. Full-scan electron impact spectra across the mass range of m/z 50–700 were acquired in each run and the final spectra were obtained after background correction.

### SPECTRAL BINDING TITRATIONS

Binding assays of rat CYP24A1 with 3-epi-1α,25$(OH)_2D_3$ and 1α,25$(OH)_2D_3$ were performed using a Cary Model 500 double-beam spectrophotometer as described [Annalora et al., 2004]. Vitamin D substrates were prepared in 4.5% (2-hydroxypropyl)-β-cyclodextrin and added to a solution of purified CYP24A1 (0.3 μM) in 1.0 ml of 100 mM phosphate buffer (pH 7.4). The stability and concentration of purified enzyme were determined by CO-difference spectra [Omura and Sato, 1964] prior to each titration. All spectral spin-state titrations were taken to saturation with tenfold substrate excess. The apparent dissociation constant ($K_d$) of 3-epi-1α,25$(OH)_2D_3$ or 1α,25$(OH)_2D_3$ was estimated from the slope of titration curves of 1/r versus $1/A_{free}$, where r and $A_{free}$ represent the molar ratio of the total substrate bound to the total amount of enzyme and the free substrate concentration, respectively [Annalora et al., 2004].

### MOLECULAR DOCKING SIMULATIONS USING AUTODOCK 4.2

The simulated docking of 3-epi-1α,25$(OH)_2D_3$ into the substrate-free, crystal structure of rat CYP24A1 (PDB code 3K9V, copy A) was performed according to a crystal structure-calibrated docking protocol as described [Annalora et al., 2010; Rhieu et al., 2011]. The topology and parameters of ligands were generated using the PRODRG server [Schuttelkopf and van Aalten, 2004] and used as input files for AutoDock 4.2 [Goodsell and Olson, 1990].

### STATISTICAL ANALYSIS

Analysis of variance with Student's *t*-test was used to analyze the experimental data. $P < 0.05$ was considered to indicate statistically significant differences between the control and experimental groups.

## RESULTS

### IDENTIFICATION OF VARIOUS LIPID-SOLUBLE METABOLITES OF 3-EPI-1α,25$(OH)_2D_3$ AND 1α,25$(OH)_2D_3$ PRODUCED BY AN ISOLATED PERFUSED RAT KIDNEY

We studied the metabolic fates of both 3-epi-1α,25$(OH)_2D_3$ and 1α,25$(OH)_2D_3$ using the technique of an isolated perfused rat kidney. The kidney perfusions were performed with 1 μM concentration of each compound and the lipid extracts of the total perfusate were analyzed by HPLC as described in methods section. The HPLC profiles of the lipid extracts from a single set of kidney perfusions are shown in panels A and B of Figure 2. As shown in Figure 2A, 3-epi-1α,25$(OH)_2D_3$ was metabolized into four polar metabolites (peaks 1*–4*), all of which exhibited the typical vitamin D chromophore showing $\lambda_{max}$ at 265 nm and $\lambda_{min}$ at 228 nm (data not shown). The structural identity of each peak was confirmed by GC-MS and the peaks 1*–4* were identified as 3-epi-1α,25$(OH)_2$-24-oxo-$D_3$ (1*), 3-epi-1α,23$(OH)_2$-24,25,26,27-tetranor-$D_3$ (2*), 3-epi-1α,23,25$(OH)_3$-24-oxo-$D_3$ (3*), and 3-epi-1α,24,25$(OH)_3D_3$ (4*). The mass spectra were identical to those published in a previous study [Kusudo et al., 2004] and the key fragment ions of all the metabolites are summarized in Table I. The HPLC profile of the lipid extract from a control kidney perfusion with 1α,25$(OH)_2D_3$ is shown in Figure 2B. As expected, 1α,25$(OH)_2D_3$ was metabolized into four polar metabolites (peaks 1–4), all of which exhibited the typical vitamin D chromophore showing $\lambda_{max}$ at 265 nm and $\lambda_{min}$ at 228 nm (data not shown). Peaks 1–4 were identified as 1α,25$(OH)_2$-24-oxo-$D_3$ (1), 1α,23$(OH)_2$-24,25,26,27-tetranor-$D_3$ (2), 1α,23,25$(OH)_3$-24-oxo-$D_3$ (3), and 1α,24,25$(OH)_3D_3$ (4) based on co-migration with known standards. Based on these results, it became clear that both 3-epi-1α,25$(OH)_2D_3$ and 1α,25$(OH)_2D_3$ were metabolized by the isolated perfused rat kidney into similar daughter metabolites produced through the C-24 oxidation pathway.

### RELATIVE AMOUNTS OF THE LIPID-SOLUBLE METABOLITES OF 3-EPI-1α,25$(OH)_2D_3$ AND 1α,25$(OH)_2D_3$ PRODUCED BY AN ISOLATED PERFUSED RAT KIDNEY

The amounts of unmetabolized 3-epi-1α,25$(OH)_2D_3$ and 1α,25$(OH)_2D_3$ remained in the perfusate along with all lipid-soluble metabolites produced by the kidney were calculated from the areas of their corresponding HPLC peaks. The pooled results from three kidney perfusions for each compound were compared as shown in panels C and D of Figure 2. It was noted that the amount of unmetabolized 3-epi-1α,25$(OH)_2D_3$ was almost similar to that of 1α,25$(OH)_2D_3$ while the amount of total lipid-soluble metabolites of 3-epi-1α,25$(OH)_2D_3$ was approximately twofold higher than the amount of the corresponding total lipid-soluble metabolites of 1α,25$(OH)_2D_3$ (Fig. 2C). This finding clearly indicates that the metabolic stability of 3-epi-1α,25$(OH)_2D_3$ over 1α,25$(OH)_2D_3$ does not manifest itself at the level of the starting substrate, but rather at the level of its intermediary metabolites. We then compared the amount of each individual intermediary metabolite of 3-epi-1α,25$(OH)_2D_3$ with the corresponding intermediary metabolite of 1α,25$(OH)_2D_3$. As shown in panel D of Figure 2, the amounts of all three major lipid-soluble metabolites of 3-epi-1α,25$(OH)_2D_3$, namely 3-epi-1α,24,25$(OH)_3D_3$, 3-epi-1α,25$(OH)_2$-24-oxo-$D_3$, and 3-epi-1α,23,25$(OH)_3$-24-oxo-$D_3$, were higher than the corresponding lipid-soluble metabolites of 1α,25$(OH)_2D_3$. On the contrary, the amount of 3-epi-1α,23$(OH)_2$-24,25,26,27-tetranor-$D_3$, the side-chain cleaved lipid-soluble metabolite of 3-epi-1α,25$(OH)_2D_3$ was significantly lower than that of 1α,23$(OH)_2$-24,25,26,27-tetranor-$D_3$, the side-chain cleaved lipid-soluble metabolite of 1α,25$(OH)_2D_3$. This finding indicates that the addition of 3-epi modification to 1α,25$(OH)_2D_3$ delays the process of side-chain cleavage between C-23 and C-24, which is involved in the metabolic conversion of 3-epi-1α,23,25$(OH)_3$-24-oxo-$D_3$ into 3-epi-1α,23$(OH)_2$-24,25,26,27-tetranor-$D_3$, leading to its final inactivation at a slower rate as compared to 1α,25$(OH)_2D_3$. To provide further proof to these findings, we decided to compare the amount of the final water-soluble metabolite produced from 3-epi-1α,25$(OH)_2D_3$ with that of 1α,25$(OH)_2D_3$. However, based on our previous experience, we recognized that the process of isolation and purification of water-soluble metabolites of vitamin D compounds from kidney perfusate is quite arduous due to a high degree of background interferences. Therefore, we resorted to an alternate approach of using purified rat CYP24A1 in a cell-free reconstituted system to quantitate the relative

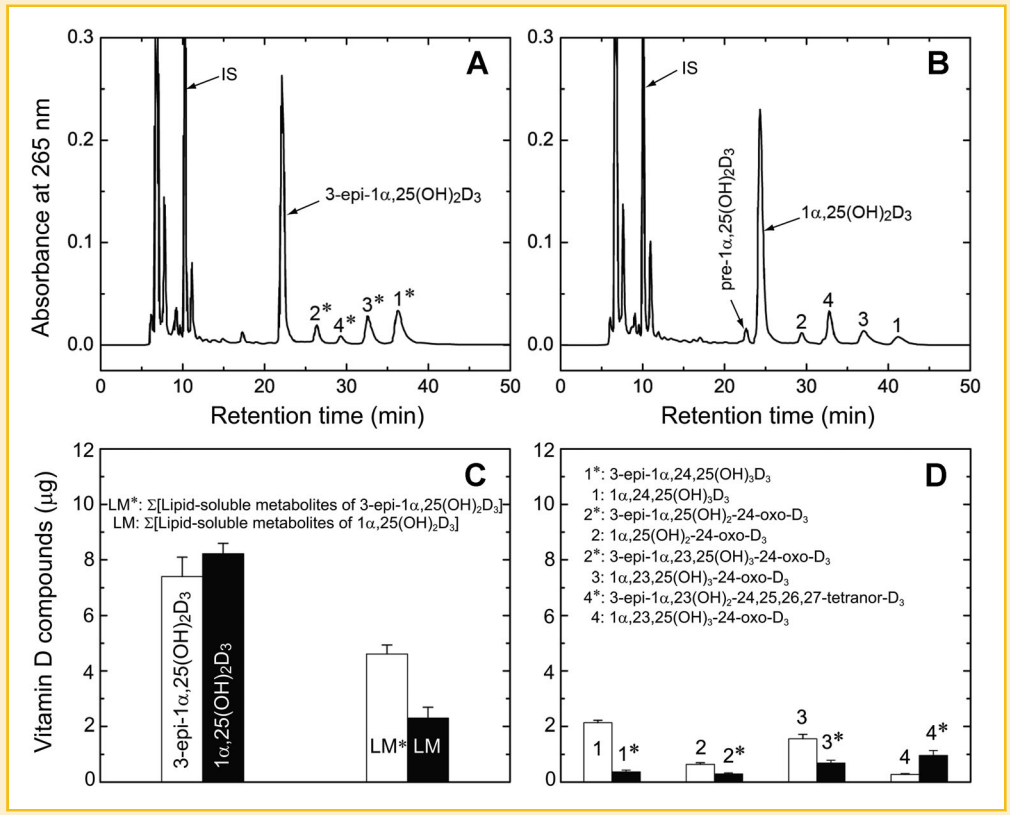


**Fig. 2.** HPLC chromatograms of the lipid extract of 50 ml perfusate obtained by perfusing an isolated rat kidney for 2 h with 1 $\mu$M of (A) 3-epi-1α,25(OH)$_2$D$_3$ and (B) 1α,25(OH)$_2$D$_3$. 25(OH)D$_3$ (IS) was added to each sample before lipid extraction as internal standard to quantify the efficiency of the extraction step. Peaks were numbered according to the order of metabolites produced through the C-24 oxidation pathway: (A) 1*, 3-epi-1α,24,25(OH)$_3$D$_3$; 2*, 3-epi-1α,25(OH)$_2$-24-oxo-D$_3$; 3*, 3-epi-1α,23,25(OH)$_3$-24-oxo-D$_3$; 4*, 3-epi-1α,23(OH)$_2$-24,25,26,27-tetranor-D$_3$; (B) 1, 1α,24,25-trihydroxyvitamin D$_3$ (1α,24,25(OH)$_3$D$_3$); 2, 1α,25-dihydroxy-24-oxo-vitamin D$_3$ (1α,25(OH)$_2$-24-oxo-D$_3$); 3, 1α,23,25-trihydroxy-24-oxo-vitamin D$_3$ (1α,23,25(OH)$_3$-24-oxo-D$_3$); 4, 1α,23-dihydroxy-24,25,26,27-tetranor-vitamin D$_3$ (1α,23(OH)$_2$-24,25,26,27-tetranor-D$_3$). C: The amounts of unmetabolized parent substrates (open bar, 3-epi-1α,25(OH)$_2$D$_3$; closed bar, 1α,25(OH)$_2$D$_3$) and their respective lipid-soluble metabolites produced in rat kidneys. Error bars indicate the SE of three independent experiments.

amounts of the water-soluble metabolites produced from 3-epi-1α,25(OH)$_2$D$_3$ and 1α,25(OH)$_2$D$_3$.

### RELATIVE AMOUNTS OF THE WATER-SOLUBLE METABOLITES OF 3-EPI-1α,25(OH)$_2$D$_3$ AND 1α,25(OH)$_2$D$_3$ PRODUCED BY RAT CYP24A1

We first performed several preliminary incubations using a rat CYP24A1 reconstituted system in an attempt to find the optimal incubation conditions needed for the best yield of water-soluble metabolites of 1α,25(OH)$_2$D$_3$ and 3-epi-1α,25(OH)$_2$D$_3$. After optimizing the concentrations of ADR, ADX, and NADPH, we incubated either 3-epi-1α,25(OH)$_2$D$_3$ or 1α,25(OH)$_2$D$_3$ with purified rat CYP24A1 at a final concentration of 5 $\mu$M for 25 min. Five separate incubations were performed for each compound using identical incubation conditions. Both lipid- and water-soluble metabolites from each incubation mixture were extracted into two separate extracts (extract #1 and #2) as described in methods section. Based on the results obtained from the HPLC analysis of extract #1 containing unmetabolized substrates and the lipid-soluble metabolites, we arrived at the same conclusions as those obtained from our previous experiments using the isolated perfused kidneys (data not shown).

TABLE I. Fragment Ions of 3-Epi-1α,25(OH)$_2$D$_3$ Metabolites Produced in Rat Kidney

| | Mass spectral analysis (m/z) | | |
|---|---|---|---|
| Metabolite[a] | Molecular ion | Other ions | Structural identity |
| 1* | 720 | 131, 217, 589 | 3-epi-1α,24,25(OH)$_3$D$_3$ |
| 2* | 646 | 131, 217, 515 | 3-epi-1α,25(OH)$_2$-24-oxo-D$_3$ |
| 3* | 734 | 131, 217, 603, 644 | 3-epi-1α,23,25(OH)$_3$-24-oxo-D$_3$ |
| 4* | 576 | 131, 147, 217 | 3-epi-1α,23(OH)$_2$-24,25,26,27-tetranor-D$_3$ |

[a]Each metabolite was subjected to trimethylsilyl derivatization.

The HPLC profiles resulting from the analysis of the extract #2 containing water-soluble metabolites are shown in Figure 3. As shown in panel A, the HPLC peak designated as X* exhibited the characteristic UV chromophore of vitamin D showing $\lambda_{max}$ at 265 nm and $\lambda_{min}$ at 228 nm (shown in the inset) and this peak was tentatively identified as 3-epi calcitroic acid, the putative water-soluble metabolite of 3-epi-1α,25$(OH)_2D_3$. Likewise, as shown in panel B, the HPLC peak designated as X exhibited the characteristic UV chromophore of vitamin D showing $\lambda_{max}$ at 265 nm and $\lambda_{min}$ at 228 nm (shown in the inset) and this peak was previously identified as calcitroic acid, the water-soluble metabolite of 1α,25$(OH)_2D_3$. The amounts of water-soluble metabolites of 3-epi-1α,25$(OH)_2D_3$ and 1α,25$(OH)_2D_3$ produced by rat CYP24A1 were calculated from the areas of their corresponding HPLC peaks. The adjustments for their recovery were made according to the recovery of cholacalcioic acid which was added to the incubation mixture prior to lipid extraction. The pooled results from five separate incubations for each compound were compared as shown in Figure 3C. The amount of the water-soluble metabolite of 3-epi-1α,25$(OH)_2D_3$ was approximately threefold lower than that the water-soluble metabolite of 1α,25$(OH)_2D_3$. This finding indicates that the metabolic stability of 3-epi-1α,25$(OH)_2D_3$ over 1α,25$(OH)_2D_3$ is at the final metabolic step in its conversion into water-soluble metabolite through the C-24 oxidation pathway.

### IDENTIFICATION OF THE WATER-SOLUBLE METABOLITE OF 3-EPI-1α,25$(OH)_2D_3$ AS 3-EPI-CALCITROIC ACID

The identification of the water-soluble metabolite of 3-epi-1α,25$(OH)_2D_3$ has not been achieved to date, even though it has been speculated to be structurally analogous to calcitroic acid, the water-soluble metabolite of 1α,25$(OH)_2D_3$. In the current study, we obtained both the water-soluble metabolites X* and X in a quantity sufficient for their structure identification by performing several more incubations using the rat CYP24A1 reconstituted system as described in the previous section. The metabolites X* and X were further purified prior to trimethylsilyl (TMS) derivatization followed by GC/MS analysis. As shown in Figure 4A, the trimethylsilylated metabolite X* ($X^*_{TMS}$) exhibited a molecular ion ($[M^+]$) at m/z 590 followed by the sequential losses of trimethylsilanol moieties (90 Da) to produce the fragments at m/z 500 and m/z 410. The characteristic fragment ions at m/z 217 and m/z 459 ($[M-131]^+$) were derived from A-ring cleavage. The fragment ion at m/z 117 was produced due to the loss of the TMS-derivatized COOH group and this finding accounts for the presence of a TMS ester function in the side-chain of X*. As shown in Figure 4B, the mass spectrum of trimethylsilylated metabolite ($X^*_{TMS}$) is virtually identical to that of $X_{TMS}$. However, as expected the GC retention time for $X^*_{TMS}$ ($t_R = 22.97$ min) is different from that of $X_{TMS}$ ($t_R = 22.05$ min). Thus, we identified unequivocally the water-soluble metabolite of 3-epi-1α,25$(OH)_2D_3$ as 3-epi-calcitroic acid.

### SUBSTRATE-BINDING PROPERTIES OF CYP24A1

Binding of 3-epi-1α,25$(OH)_2D_3$ or 1α,25$(OH)_2D_3$ to CYP24A1 induced a Type-I spectral change (data not shown), indicating the spin state of heme iron of CYP24A1 is changed from low (S = 1/2) to high (S = 5/2). The preference of CYP24A1 for 1α,25$(OH)_2D_3$ over 3-epi-1α,25$(OH)_2D_3$ was evident from its apparent $K_d$ value of 0.036 μM, which is

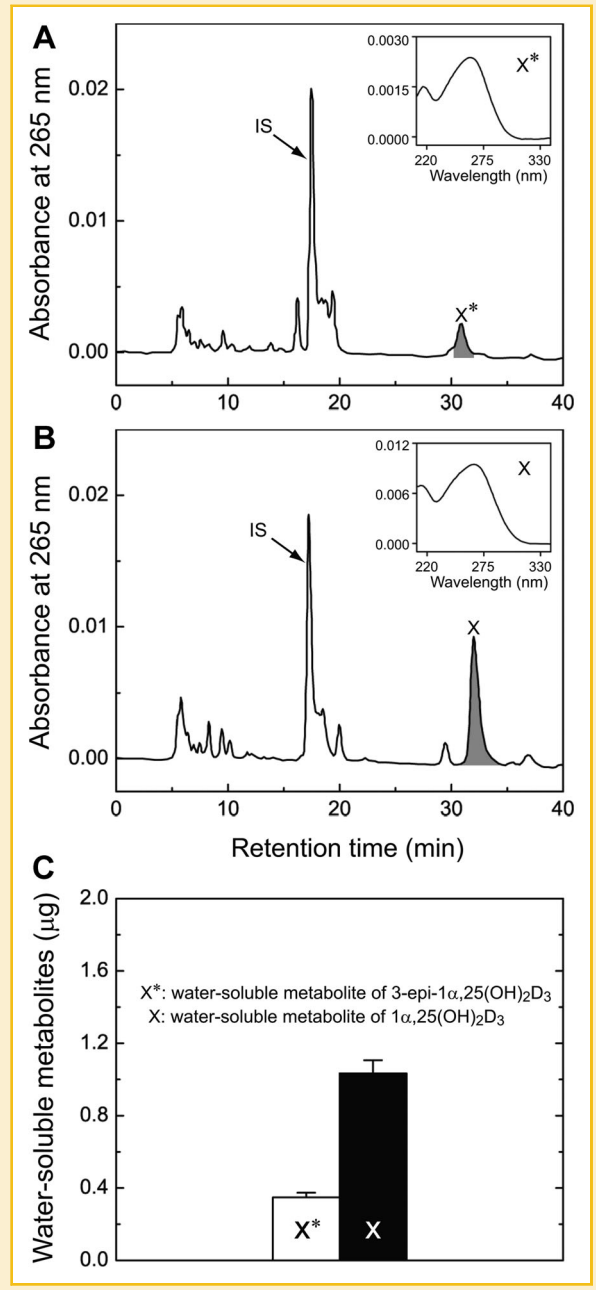


**Fig. 3.** HPLC chromatograms of water-soluble metabolites of 3-epi-1α,25$(OH)_2D_3$ (panel A) and1α,25$(OH)_2D_3$ (panel B) produced by rat CYP24A1 in a reconstituted system. Prior to extraction, cholacalcioic acid (IS) was added to each sample as an internal standard to quantify the efficiency of the extraction of water-soluble metabolites. Peaks X* and X (shaded in gray) were collected and subjected to GC-MS analysis. The UV spectra of peaks X* and X showing the characteristic vitamin $D_3$ chromophore ($\lambda_{max}$ at 265 nm; $\lambda_{min}$ at 228 nm) are provided in insets of panel A and panel B, respectively. Panel C: Relative amounts of water-soluble metabolites of 3-epi-1α,25$(OH)_2D_3$ and 1α,25$(OH)_2D_3$ produced in CYP24A1 reconstitution systems containing 5 μM substrate, 0.5 μM ADR, 0.5 μM ADX, 0.5 μM CYP24A1, and 1 mM NADPH. The reaction mixture was incubated at 37°C for 25 min. Metabolites were quantified by integrating the area of the ultraviolet peaks at an absorbance of 265 nm. Error bars represent the SD of five replicates.

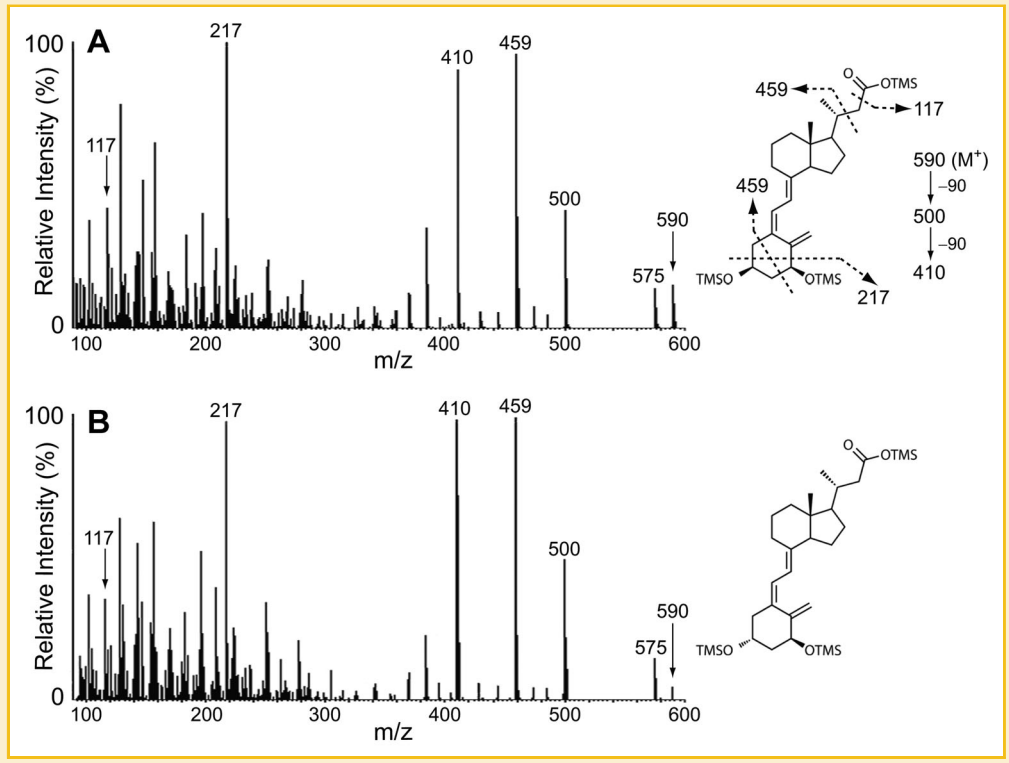


**Fig. 4.** Mass spectra of trimethylsilyl derivatives of major water-soluble metabolite of (A) 3-epi-1α,25(OH)$_2$D$_3$ and (B) 1α,25(OH)$_2$D$_3$ produced by rat CYP24A1 in a reconstituted system.

approximately fourfold lower than that of 3-epi-1α,25(OH)$_2$D$_3$ (Table II).

### DOCKING ANALYSIS

We conducted a computational docking simulation using the crystal structure of CYP24A1 to explore further how C-3 epimerization of 1α,25(OH)$_2$D$_3$ alters the nature of its binding to CYP24A1. Docking results obtained here for 3-epi-1α,25(OH)$_2$D$_3$ were compared to those previously reported for 1α,25(OH)$_2$D$_3$ [Rhieu et al., 2011]. As shown in Figure 5, 3-epi-1α,25(OH)$_2$D$_3$ docks the active site of CYP24A1 almost perpendicular to the heme plane, in a novel configuration stabilized heavily by hydrophobic contacts from the ligand's C-18, C-19, and C-21 methyl groups. In this configuration, the 3α-OH group interacts with conserved residue L129 (B/C loop) rather than T395 (β1-4), preventing the hormone's A-ring from swiveling fully into the binding pocket. Interestingly, even though this binding defect alters the terminal positioning of the 1α-OH group and restricts the rotational freedom of the CD-ring; the proper recognition of the side-chain is still allowed. In this strained configuration, the C-21 methyl group of 3-epi-1α,25(OH)$_2$D$_3$ is better positioned to form a hydrophobic contact with the B/C loop (i.e., M148), than to perturb a theoretical water molecule bound to the low-spin heme iron, which could alter its ability to trigger the enzyme's catalytic mechanism [Annalora et al., 2010]. Because of this alternative docking configuration, the computed ligand dissociation constant ($K_I$) for 3-epi-1α,25(OH)$_2$D$_3$ is increased over 30-fold compared to 1α,25(OH)$_2$D$_3$ (Table III). This finding suggests that C-3 epimerization of 1α,25(OH)$_2$D$_3$ dramatically reduces its binding affinity to CYP24A1.

TABLE II. Substrate-Binding Properties of Rat CYP24A1 for 3-Epi-1α,25(OH)$_2$D$_3$ and 1α,25(OH)$_2$D$_3$

| Substrate | Spectral perturbation[a,b] | Dissociation constant ($K_d$)[b] (μM) |
|---|---|---|
| 3-epi-1α,25(OH)$_2$D$_3$ | 0.007 (0.001) | 0.144 (0.032) |
| 1α,25(OH)$_2$D$_3$ | 0.032 (0.002) | 0.036 (0.004) |

[a]$\Delta Abs_{max} - \Delta Abs_{free}$, where $\Delta Abs_{max}$ is the maximal change in absorbance between 417 and 392 nm during each titration, and $\Delta Abs_{free}$ is the initial difference in absorbance between 417 and 392 nm for the free enzyme prior to each titration. Spectral perturbation reflects the substrate-binding efficiency within the active site of CYP24A1; greater perturbation is correlated to more efficient binding.
[b]Data represent the mean (SD) of four replicates.

## DISCUSSION

In some endocrine systems, C-3 epimerization is known to play a pivotal role in hormone inactivation as seen in the conversion of 5α-dihydrotestosterone, a potent steroid hormone into its inactive form, 3α-androstanediol [Penning et al., 1997]. C-3 epimerization has also been observed in vitamin D endocrine system [Reddy et al., 1994], where the hormonal form 1α,25(OH)$_2$D$_3$ is converted into its C-3 epimer, 3-epi-1α,25(OH)$_2$D$_3$. Unlike the role of C-3 epimerization as an inactivation process noted in the case of steroid 5α-

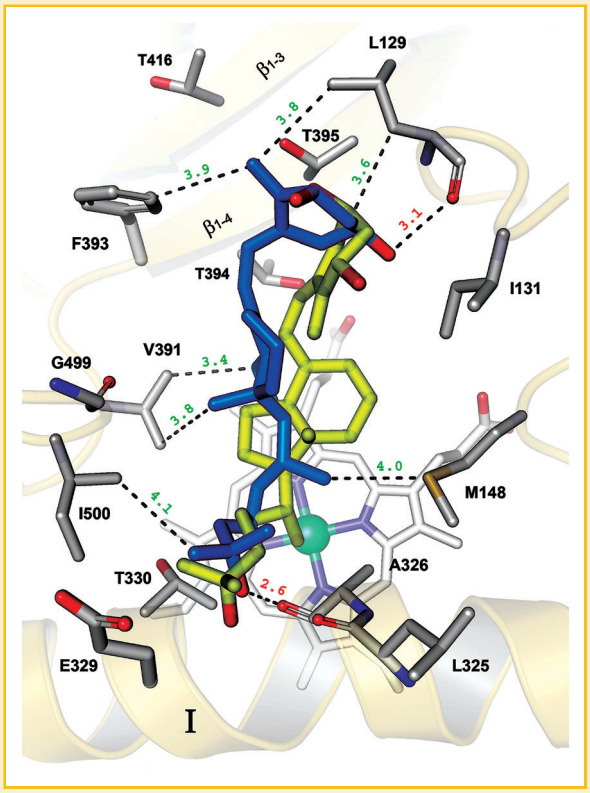


Fig. 5. Computational docking analysis of 3-epi-1α,25(OH)$_2$D$_3$ in the active site of rat CYP24A1. Low-energy docking solutions for 3-epi-1α,25(OH)$_2$D$_3$ (shown in light blue) are superimposed with a control docking solution for 1α,25(OH)$_2$D$_3$ (shown in yellow) that was previously reported [Rhieu et al., 2011]. Key amino acid residues that define the substrate-binding pocket in CYP24A1 are depicted and important hydrogen (Å, red) and hydrophobic (Å, green) bond distances are noted. C-3 epimerization diminished the computed binding affinity for 1α,25(OH)$_2$D$_3$ over 30-fold, causing 3-epi-1α,25(OH)$_2$D$_3$ to bind the active site in a pitched configuration that limits substrate recognition and may render the metabolism of 3-epi-1α,25(OH)$_2$D$_3$ by CYP24A1 to occur at a slower rate than 1α,25(OH)$_2$D$_3$.

dihydrotestosterone, 3-epi-1α,25(OH)$_2$D$_3$ was found to be almost as potent as 1α,25(OH)$_2$D$_3$ in various biological activities [Norman et al., 1993; Schuster et al., 1997; Brown et al., 1999; Nakagawa et al., 2001; Rehan et al., 2002; Furigay and Swamy, 2004; Sakurai et al., 2009; Molnár et al., 2011]. This intriguing finding gained further attention in that 3-epi-1α,25(OH)$_2$D$_3$ exhibits less calcemic activity when compared to 1α,25(OH)$_2$D$_3$ [Morrison and Eisman, 1991; Norman et al., 1993; Fleet et al., 1996]. The lowering of calcemic activity of vitamin D compounds due to C-3 epimerization was exemplified by 3-epi-1α-hydroxyvitamin D$_3$, a potent vitamin D analog whose threshold dose for the development of hypercalcemia was nearly 80-fold higher than its parent compound, 1α-hydroxyvitamin D$_3$ [Brown et al., 2005].

It was also noted that C-3 epimerization of 1α,25(OH)$_2$D$_3$ results in reduced binding affinity for the VDR [Norman et al., 1993]. However, some of biological activities of 3-epi-1α,25(OH)$_2$D$_3$ appear to be little affected by low binding affinity for the VDR [Brown et al., 1999; Harant et al., 2000]. Following these observations, the crystal structure of human VDR complexed with 3-epi-1α,25(OH)$_2$D$_3$ [Molnár et al., 2011] revealed that 3-epi-1α,25(OH)$_2$D$_3$ lacks interaction with S278, which is one of key residues involved in ligand recognition by the VDR [Choi et al., 2001]. However, it is interesting to note that 3-epi-1α,25(OH)$_2$D$_3$ maintains the number of hydrogen bonds by an alternative water-mediated interaction to compensate the abolished interaction with S278 [Molnár et al., 2011]. Despite these findings, the underlying mechanisms by which the biological activities of 3-epi-1α,25(OH)$_2$D$_3$ are exerted still remain elusive. Two decades ago, it was shown for the first time that the addition of a single structural modification to the A-ring of 1α,25(OH)$_2$D$_3$ as in the case of 1α-(hydroxymethyl)-25(OH)-D$_3$ renders 1α,25(OH)$_2$D$_3$ resistant to CYP24A1-mediated metabolism [Posner et al., 1993]. This finding led us to hypothesize that C-3 epimerization of 1α,25(OH)$_2$D$_3$ may also render 1α,25(OH)$_2$D$_3$ resistant to CYP24A1-mediated metabolism in a way similar to 1α-(hydroxymethyl)-25(OH)-D$_3$. In support of this hypothesis, it was later observed in bovine parathyroid cells that 3-epi-1α,25(OH)$_2$D$_3$ resists its metabolism by CYP24A1 [Brown et al., 1999]. Soon after this observation, a more detailed comparative metabolism study was performed by incubating human keratinocytes with physiological concentrations of radiolabeled 3-epi-1α,25(OH)$_2$D$_3$ and 1α,25(OH)$_2$D$_3$. It was found that 3-epi-1α,25(OH)$_2$[26,27-$^3$H]D$_3$ and its lipid-soluble [$^3$H]-metabolites remained detectable in the incubations for a longer period of time than 1α,25(OH)$_2$[26,27-$^3$H]D$_3$ and its lipid-soluble [$^3$H]-metabolites [Astecker et al., 2000]. This finding for the first time suggested that 3-epi-1α,25(OH)$_2$D$_3$ and its lipid-soluble metabolites are metabolized at a slower rate when compared to 1α,25(OH)$_2$D$_3$ and its lipid-soluble metabolites. However, none of the intermediary metabolites of 3-epi-1α,25(OH)$_2$D$_3$ were identified and the findings of this study needed further confirmation. Based on these early observations, it was hypothesized that some of the noncalcemic activities of 3-epi-1α,25(OH)$_2$D$_3$ may be due to the accumulation of its long-lived intermediary metabolites.

TABLE III. Flexible Ligand Docking Results for 3-Epi-1α,25(OH)$_2$D$_3$ in the Crystal Structure of Rat CYP24A1

| Ligand[a] | Binding energy[b] (kcal/mol) | Dissociation constant ($K_I$)[c] (nM) | Occupancy[d] |
|---|---|---|---|
| 3-epi-1α,25(OH)$_2$D$_3$ | −10.07 | 41.26 | 0.25 |
| 1α,25(OH)$_2$D$_3$[e] | −12.13 | 1.29 | 0.16 |

[a]Flexible ligand docking simulations were performed using Autodock 4.2. Evaluations were based on experiments consisting of 200 Genetic Algorithm (GA) runs, long evaluations (25,000,000 evals. per GA run), using a search grid targeting the full distal surface of rat CYP24A1 (PDB code 3K9V, copy A).
[b]Binding energy is the computed value for the low-energy docking conformation in the high occupancy solution bin (root mean square = 2.0 Å).
[c]Dissociation constant or inhibition constant ($K_I$) is the computed nanomolar affinity for the low-energy, active site binding solution with the highest occupancy.
[d]Occupancy refers to the fraction of total docking solutions represented by the low-energy active site docking solution (root mean square = 2.0 Å).
[e]Computed ligand docking properties for 1α,25(OH)$_2$D$_3$ were published previously [Rhieu et al., 2011]. Results are reproduced here to aid comparison.

We now provide clear evidence in support of the above hypothesis by performing careful comparative metabolism studies between 3-epi-1α,25(OH)$_2$D$_3$ and 1α,25(OH)$_2$D$_3$ using both the technique of isolated rat kidney perfusion and purified rat CYP24A1 in a cell-free reconstituted system. We confirmed that 3-epi-1α,25(OH)$_2$D$_3$ is metabolized in the rat mainly through the C-24 oxidation pathway by identifying all the major lipid-soluble intermediary metabolites of 3-epi-1α,25(OH)$_2$D$_3$ produced by the perfused rat kidney and 3-epi calcitroic acid produced by the rat CYP24A1. In other studies, it was noted that 3-epi-1α,25(OH)$_2$D$_3$ is also metabolized through the C-23 oxidation pathway resulting in the formation of 3-epi-1α,23,25-trihydroxyvitamin D$_3$ (3-epi-1α,23,25(OH)$_3$D$_3$) and other minor metabolites as shown in Figure 6. However, we did not detect any production of 3-epi-1α,23,25(OH)$_3$D$_3$ or 1α,23,25(OH)$_3$D$_3$ by the isolated rat kidneys when perfused with their respective parent substrates at a concentration of 1 μM while the production of these metabolites was detectable only when perfused with the same substrates at a concentration of 5 μM (data not shown). Interestingly, human keratinocytes, unlike the perfused rat kidneys, produced both 3-epi-1α,23,25(OH)$_3$D$_3$ and 1α,23,25(OH)$_3$D$_3$ when incubated with their respective parent substrates at a concentration of 1 μM [Reddy et al., 2001]. These observations are due to the species-based differences that were well-documented in previous studies dealing with the differences between rat and human CYP24A1-mediated metabolism of 1α,25(OH)$_2$D$_3$. For example, rat CYP24A1 metabolizes 1α,25(OH)$_2$D$_3$ mainly through the C-24 oxidation pathway while human CYP24A1 metabolizes 1α,25(OH)$_2$D$_3$ through both C-24 and C-23 oxidation pathways [Engstrom et al., 1986; Beckman et al., 1996; Sakaki et al., 1999, 2000; Kusudo et al., 2004]. The important contribution of our present study was to identify for the first time the final water-soluble metabolite of 3-epi-1α,25(OH)$_2$D$_3$ produced by rat CYP24A1 unequivocally as 3-epi-calcitroic acid (Figs. 4 and 6). Furthermore, we found that the amount of 3-epi-calcitroic acid produced from 3-epi-1α,25(OH)$_2$D$_3$ was approximately threefold lower than that of calcitroic acid produced from 1α,25(OH)$_2$D$_3$ under identical incubation conditions (Fig. 3C). This finding indicated that the rate of overall side-chain oxidation of 3-epi-1α,25(OH)$_2$D$_3$ by CYP24A1, leading to its final conversion into 3-epi-calcitroic acid, is slower than that of 1α,25(OH)$_2$D$_3$.

In support of the results obtained from our comparative metabolism studies between 3-epi-1α,25(OH)$_2$D$_3$ and 1α,25(OH)$_2$D$_3$, we also performed comparative ligand-binding assays and molecular-docking studies. First, the binding studies indicated that the apparent K$_d$ value for 3-epi-1α,25(OH)$_2$D$_3$ was approximately fourfold higher than that for 1α,25(OH)$_2$D$_3$. This means that the conditions for the formation of enzyme-substrate complexes for 3-epi-1α,25(OH)$_2$D$_3$ are less favorable in comparison to 1α,25(OH)$_2$D$_3$ (Table II). This finding is in a good agreement with the results from a previous study which provided apparent K$_m$ values of 0.15 and 0.06 μM for the initial C24-hydroxylation by CYP24A1 towards 3-epi-1α,25(OH)$_2$D$_3$ and 1α,25(OH)$_2$D$_3$, respectively [Kusudo et al., 2004]. In addition, we explored the structural basis for the enhanced metabolic stability of 3-epi-1α,25(OH)$_2$D$_3$ over 1α,25(OH)$_2$D$_3$ via a computational docking simulation using the crystal structure of rat CYP24A1. The open crystal structure of CYP24A1 has been offering a unique template for studying pre-catalytic substrate binding events [Annalora et al., 2010; Rhieu et al., 2011]. In our previous study, we noted that the susceptibility of a vitamin D compound to CYP24A1-mediated oxidation depends mainly upon the proper docking of its 25-hydroxylated side-chain and, to a lesser extent, the CD-ring [Rhieu et al., 2011]. Such trends persist in the current study, as 3-epi-1α,25(OH)$_2$D$_3$ displays relatively normal side-

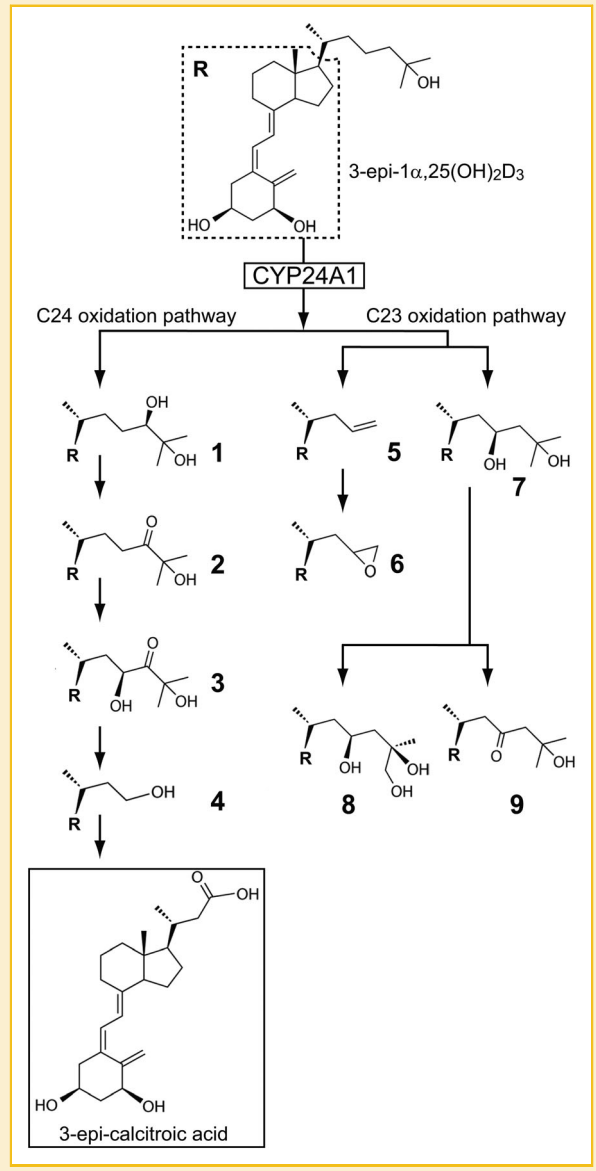


**Fig. 6.** A comprehensive metabolism of 3-epi-1α,25(OH)$_2$D$_3$ by CYP24A1. Shown are the previously determined structures of 3-epi-1α,25(OH)$_2$D$_3$ metabolites produced by human CYP24A1 and rat CYP24A1 [Kusudo et al., 2004]. Metabolites are designated *1* to *8*: *1*, 3-epi-1α,24,25-trihydroxyvitamin D$_3$; *2*, 3-epi-1α,25-dihydroxy-24-oxo-vitamin D$_3$; *3*, 3-epi-1α,23,25-trihydroxy-24-oxo-vitamin D$_3$; *4*, 3-epi-1α,23-dihydroxy-24,25,26,27-tetranor-vitamin D$_3$; *5*, 3-epi-25,26,27-trinor-23-ene-1α-hydroxyvitamin D$_3$; *6*, 3-epi-25,26,27-trinor-23,24-epoxide-1α-hydroxyvitamin D$_3$; *7*, 3-epi-1α,23,25-trihydroxyvitamin D$_3$; *8*, 3-epi-1α,23,26-trihydroxyvitamin D$_3$; *9*, 3-epi-1α,25-dihydroxy-23-oxo-vitamin D$_3$. 3-epi-calcitroic acid was isolated in this study as a major side-chain cleaved water-soluble metabolite of 3-epi-1α,25(OH)$_2$D$_3$.

chain docking with respect to 1α,25(OH)$_2$D$_3$ (Fig. 5). Unlike other vitamin D compounds previously studied [Rhieu et al., 2011], 3-epi-1α,25(OH)$_2$D$_3$ docks the active site of CYP24A1 in a novel conformation that alters significantly the accessibility of the A-ring and CD-ring to the active site without disrupting its ability to dock the side-chain properly over the heme. These results indicate that the active site of CYP24A1 can still accommodate 3-epi-1α,25(OH)$_2$D$_3$ although it is highly selective in general for vitamin D compounds possessing the 3β-OH group. Thus, C-3 epimerization appears to alter the recognition of the secosteroid nucleus but not the side-chain, which would partially explain how 3-epi-1α,25(OH)$_2$D$_3$ still remains to be susceptible to CYP24A1-mediated metabolism, despite its diminished spectral and computational binding properties towards CYP24A1 (Tables II and III). In short, we conclude that 3-epi-1α,25(OH)$_2$D$_3$, with the epimerized hydroxyl group at C-3, achieves its enhanced metabolic stability by binding CYP24A1 in an alternative configuration that diminishes its active site recognition and/or retention time sufficiently to slow the overall rate of side-chain oxidation.

Based on the insights gained from both metabolism and docking studies, it appears that the enhanced metabolic stability of 3-epi-1α,25(OH)$_2$D$_3$ manifests itself mainly at the level of its daughter metabolites, especially the 24-oxo metabolites (Fig. 2). In this regard, the metabolism of 3-epi-1α,25(OH)$_2$D$_3$ by CYP24A1 is comparatively similar to that of synthetic analogs of 1α,25(OH)$_2$D$_3$ which are discussed later. Our own interest in 24-oxo metabolites of different vitamin D compounds started three decades ago with the isolation and identification of 23,25(OH)$_2$-24-oxo-D$_3$ [Reddy et al., 1982b; Mayer et al., 1982, 1983a]. However, this interest was soon dampened by the findings of 1α,25(OH)$_2$-24-oxo-D$_3$ and 1α,23,25(OH)$_3$-24-oxo-D$_3$, two natural 24-oxo metabolites of 1α,25(OH)$_2$D$_3$ as having minimal calcemic activities in terms of their ability to initiate intestinal calcium absorption and bone calcium mobilization [Mayer et al., 1983b]. Almost a decade later, our interest to investigate the noncalcemic actions of the 24-oxo metabolites was rekindled with the rapid expansion of our knowledge in the various noncalcemic actions of 1α,25(OH)$_2$D$_3$ [Nagpal et al., 2005; Bouillon et al., 2008; Rosen et al., 2012]. This led us to report for the first time that 1α,23,25(OH)$_3$-24-oxo-D$_3$, the natural 24-oxo metabolite with minimal in vivo calcemic activity, suppresses parathyroid hormone secretion in primary cultures of bovine parathyroid cells with a potency equal to 1α,25(OH)$_2$D$_3$ [Lee et al., 1997]. Subsequently, we also reported that 1α,23,25(OH)$_3$-24-oxo-D$_3$ inhibits clonal growth of HL-60 cells and induces expression of CD11b protein with a potency equal to 1α,25(OH)$_2$D$_3$ [Rao et al., 2001]. Along with these studies, we and others provided a wealth of information regarding different noncalcemic actions of the 24-oxo-mtabolites of some of the highly potent synthetic analogs of 1α,25(OH)$_2$D$_3$. The structures of the analogs pertinent to our present discussion are shown in Figure 7. The analogs were shown to acquire metabolic stability due to the accumulation of

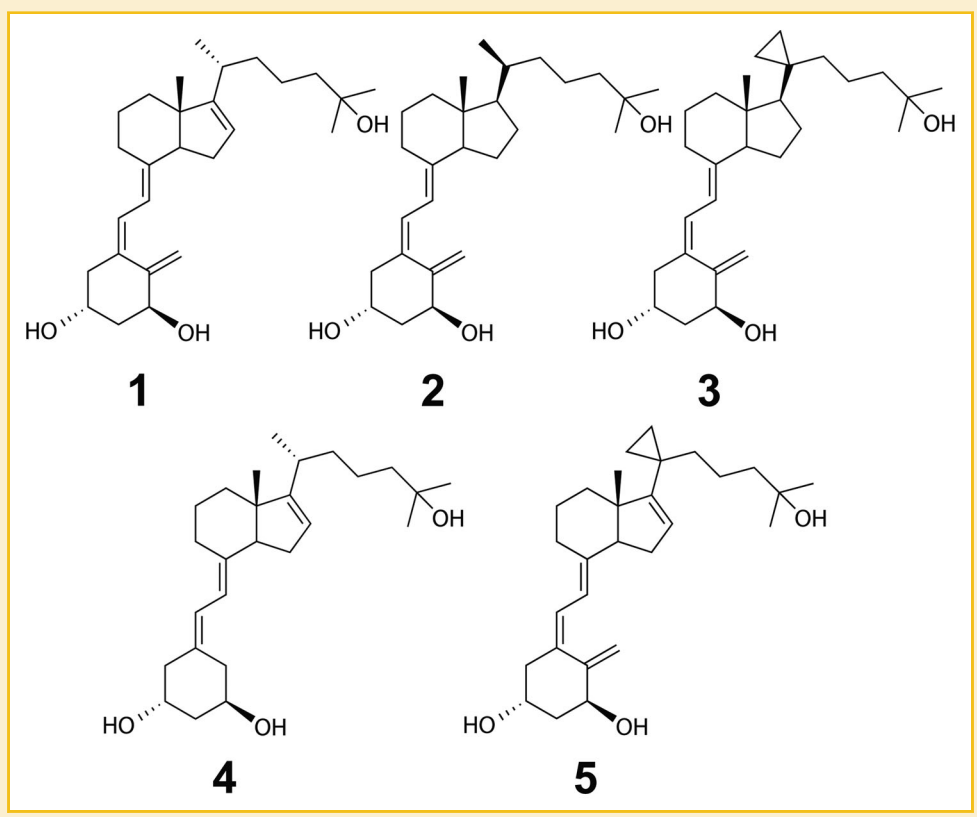


**Fig. 7.** Structures of 1α,25(OH)$_2$D$_3$ analogs that exhibit resistance to CYP24A1-mediated metabolism through the accumulation of their respective 24-oxo metabolites: *1*, 1α,25(OH)$_2$-16-ene-D$_3$; *2*, 1α,25(OH)$_2$-20-epi-D$_3$; *3*, 1α,25(OH)$_2$-20-cyclopropyl-D$_3$; *4*, 1α,25(OH)$_2$-16-ene-19-nor-D$_3$; *5*, 1α,25(OH)$_2$-16-ene-20-cyclopropyl-D$_3$.

their respective 24-oxo metabolites as a result of a block in their metabolism by CYP24A1 through the C-24 oxidation pathway. The stable 24-oxo metabolites were found to be not only equipotent to their respective parent compounds in generating different non-calcemic biological activities [Reddy et al., 1993; Lemire et al., 1994; Siu-Caldera et al., 1996; Campbell et al., 1997; Siu-Caldera et al., 1999b; Shiohara et al., 2001; Swami et al., 2003; Uskokovic et al., 2006; Laverny et al., 2009] but also consistently less calcemic when compared to their respective parent compounds. In light of the knowledge obtained through the various noncalcemic actions of the 24-oxo metabolites of both $1\alpha,25(OH)_2D_3$ and its highly potent synthetic analogs, it now becomes imperative to investigate the noncalcemic activities of the 24-oxo metabolites of 3-epi-$1\alpha,25(OH)_2D_3$ to fully comprehend the biological role of 3-epi-$1\alpha,25(OH)_2D_3$ in vitamin D endocrine system.

In summary, we provided unequivocal evidence for the metabolic stability of 3-epi-$1\alpha,25(OH)_2D_3$ over its parent, $1\alpha,25(OH)_2D_3$ through our final conclusion that the rate of overall side-chain oxidation of 3-epi-$1\alpha,25(OH)_2D_3$ by rat CYP24A1 is slower than that of $1\alpha,25(OH)_2D_3$. This conclusion is also supported by molecular docking analysis using the crystal structure of rat CYP24A1 suggesting that 3-epi-$1\alpha,25(OH)_2D_3$, unlike $1\alpha,25(OH)_2D_3$, binds to CYP24A1 in an alternate configuration that destabilizes the formation of the enzyme-substrate complex sufficiently to slow the rate at which 3-epi-$1\alpha,25(OH)_2D_3$ is inactivated by CYP24A1. We now propose that some of the noncalcemic actions of 3-epi-$1\alpha,25(OH)_2D_3$ may be attributed to its metabolic stability mainly through the accumulation of its 24-oxo metabolites.

## ACKNOWLEDGMENTS

This work which was initiated in Dr. Satya Reddy's previous laboratory at Women and Infant's Hospital was finally completed at Epimer LLC and School of Engineering, Brown University. The support for this work was provided by grants from National Institutes of Health (DK 52488), Epimer LLC, Teijin Pharma Ltd., the National Cancer Institute (1R01CA69390), and the Spanish MCI (SAF2010-15291). S.Y.R. acknowledges financial support from the National Science Foundation GK-12 Teaching Fellowship. A.J.A. acknowledges Dr. David C. Stout for providing the financial means and laboratory facilities at The Scripps Research Institute. This paper is respectfully dedicated to Dr. Milan R. Uskokovic who reported the synthesis and biological activity of a less calcemic vitamin D analog, delta 22-1,25S,26-trihydroxyvitamin $D_3$ for the first time followed by countless other novel analogs, and made them freely available to scientists all over the world. Dr. Satya Reddy is one of the many scientists who were greatly benefited by the generosity of Dr. Uskokovic, a devoted scientist, a true friend, and a great human being.

## REFERENCES

Akiyoshi-shibata M, Sakaki T, Ohyama Y, Noshiro M, Okuda K, Yabusaki Y. 1994. Further oxidation of hydroxycalcidiol by calcidiol 24-hydroxylase: A study with the mature enzyme expressed in *Escherichia coli*. Eur J Biochem 224:335–343.

Annalora AJ, Bobrovnikova-Marjon E, Serda R, Lansing L, Chiu ML, Pastuszyn A, Iyer S, Marcus CB, Omdahl JL. 2004. Rat cytochrome P450C24 (CYP24A1) and the role of F249 in substrate binding and catalytic activity. Arch Biochem Biophys 425:133–146.

Annalora AJ, Goodin DB, Hong WX, Zhang QH, Johnson EF, Stout CD. 2010. The crystal structure of CYP24A1, a mitochondrial cytochrome P450 involved in vitamin D metabolism. J Mol Biol 396:441–451.

Astecker N, Reddy GS, Herzig G, Vorisek G, Schuster I. 2000. 1α, 25-dihdyroxy-3-epi-vitamin $D_3$, a physiological metabolite of 1α,25-dihydroxyvitamin $D_3$: Its production and metabolism in primary human keratinocytes. Mol Cell Endocrinol 170:91–101.

Beckman MJ, Tadikonda P, Werner E, Prahl J, Yamada S, DeLuca HF. 1996. Human 25-hydroxyvitamin $D_3$-24-hydroxylase, a multicatalytic enzyme. Biochemistry 35:8465–8472.

Bischof MG, Siu-Caldera ML, Weiskopf A, Vouros P, Cross HS, Peterlik M, Reddy GS. 1998. Differential-related pathways of 1α,25-dihydroxycholecalciferol metabolism in human colon adenocarcinoma-derived Caco-2 cells: Production of 1α,25-dihydroxy-3-epi-cholecalciferol. Exp Cell Res 241:194–201.

Bouillon R, Okamura WH, Norman AW. 1995. Structure-function relationships in the vitamin D endocrine system. Endocr Rev 16:200–257.

Bouillon R, Carmeliet G, Verlinden L, van Etten E, Verstuyf A, Luderer HF, Lieben L, Mathieu C, Demay M. 2008. Vitamin D and human health: Lessons from vitamin D receptor null mice. Endocr Rev 29:726–776.

Brown AJ, Ritter C, Slatopolsky E, Muralidharan KR, Okamura WH, Reddy GS. 1999. 1α,25-dihydroxy-3-epi-vitamin $D_3$, a natural metabolite of 1α,25-dihydroxyvitamin $D_3$, is a potent suppressor of parathyroid hormone secretion. J Cell Biochem 73:106–113.

Brown AJ, Ritter CS, Weiskopf AS, Vouros P, Sasso GJ, Uskokovic MR, Wang G, Reddy GS. 2005. Isolation and identification of 1α-hydroxy-3-epi-vitamin $D_3$, a potent suppressor of parathyroid hormone secretion. J Cell Biochem 96:569–578.

Brumbaugh BF, Haussler MR. 1975. Nuclear and cytoplasmic binding components for vitamin D metabolites. Life Sci 16:353–362.

Campbell MJ, Reddy GS, Koeffler HP. 1997. Vitamin $D_3$ analogs and their 24—Oxo metabolites equally inhibit clonal proliferation of a variety of cancer cells but have differing molecular effects. J Cell Biochem 66:413–425.

Choi MW, Yamamoto K, Masuno H, Nakashima K, Taga T, Yamada S. 2001. Ligand recognition by the vitamin D receptor. Bioorg Med Chem 9:1721–1730.

Engstrom GW, Reinnhardt TA, Horst RL. 1986. 25-Hydroxyvitamin $D_3$-23-hydroxylase, a renal enzyme in several animal species. Arch Biochem Biophys 250:86–93.

Esvelt RP, Schnoes HK, Deluca HF. 1979. Isolation and characterization of 1α-hydroxy-23-carboxytetranorvitamin D: A major metabolite of 1,25-dihydroxyvitamin $D_3$. Biochemistry 18:3977–3983.

Fleet JC, Bradley J, Reddy GS, Ray R, Wood RJ. 1996. $1\alpha,25-(OH)_2$-vitamin $D_3$ analogs with minimal in vivo calcemic activity can stimulate significant transepithelial calcium transport and mRNA expression in vitro. Arch Biochem Biophys 329:228–234.

Furigay P, Swamy N. 2004. Anti-endothelial properties of 1,25-dihydroxy-3-epi-vitamin $D_3$, a natural metabolite of calcitriol. J Steroid Biochem Mol Biol 89–90:427–431.

Gnanaiah W, Omdahl JL. 1986. Isolation and characterization of pig kidney mitochondrial ferredoxin: $NADP^+$ oxidoreductase. J Biol Chem 261:12649–12654.

Goodsell DS, Olson AJ. 1990. Automated docking of substrates to proteins by simulated annealing. Proteins Struct Funct Bioinform 8:195–202.

Harant H, Spinner D, Reddy GS, Lindley IJD. 2000. Natural metabolites of 1α,25-dihydroxyvitamin $D_3$ retain biologic activity mediated through the vitamin D receptor. J Cell Biochem 78:112–120.

Kimura T, Parcells JH, Wang HP. 1978. Purification of adrenodoxin reductase, adrenodoxin, and cytochrome P-450 from adrenal cortex. Methods Enzymol 52:132–142.

Kusudo T, Sakaki T, Abe D, Fujishima T, Kittaka A, Takayama H, Hatakeyama S, Ohta M, Inouye K. 2004. Metabolism of A-ring diastereomers of 1α,25-dihydroxyvitamin $D_3$ by CYP24A1. Biochem Biophys Res Commun 321:774–782.

Laverny G, Penna G, Uskokovic M, Marczak S, Maehr H, Jankowski P, Ceailles C, Vouros P, Smith B, Robinson M, Reddy GS, Adorini L. 2009. Synthesis and anti-inflammatory properties of 1α,25-dihydroxy-16-ene-20-cyclopropyl-24-oxo-vitamin $D_3$, a hypocalcemic, stable metabolite of 1α,25-dihydroxy-16-ene-20-cyclopropyl-vitamin $D_3$. J Med Chem 52:2204–2213.

Lee NE, Reddy GS, Brown AJ, Williard PG. 1997. Synthesis, stereochemistry and biological activity of 1α,23,25-trihydroxy-24-oxovitamin $D_3$, a major natural metabolite of 1α,25-dihydroxyvitamin $D_3$. Biochemistry 36:9429–9437.

Lemire JM, Archer DCR, eddy GS. 1994. 1,25-Dihydroxy-24-oxo-16ene-vitamin $D_3$, a renal metabolite of the vitamin D analog 1,25-dihydroxy-16ene-vitamin $D_3$ exerts immunosuppressive activity equal to its parent without causing hypercalcemia in vivo. Endocrinology 135:2818–2821.

Makin G, Lohnes D, Byford V, Ray R, Jones G. 1989. Target cell metabolism of 1,25-dihydroxyvitamin $D_3$ to calcitroic acid: Evidence for a pathway in kidney and bone involving 24-oxidation. Biochem J 262:173–180.

Masuda S, Kamao M, Schroeder NJ, Makin HL, Jones G, Kremer R, Rhim J, Okano T. 2000. Characterization of 3-epi-1α,25-dihydroxyvitamin $D_3$ involved in 1α,25-dihydroxyvitamin $D_3$ metabolic pathway in cultured cell lines. Biol Pharm Bull 23:133–139.

Mayer E, Reddy GS, Kruse JR, Popjak G, Norman AW. 1982. Isolation and identification of 23,25-dihydroxy-24-oxo-vitamin $D_3$: A metabolite of vitamin $D_3$. Biochem Biophys Res Commun 109:370–375.

Mayer E, Reddy GS, Chandraratna RA, Okamura WH, Kruse JR, Popjàk G, Bishop JE, Norman AW. 1983a. 23,25-Dihydroxy-24-oxovitamin $D_3$: A metabolite of vitamin $D_3$ made in the kidney. Biochemistry 22:1798–1805.

Mayer E, Bishop JE, Ohnuma N, Norman AW. 1983b. Biological activity assessment of the vitamin D metabolites 1,25-dihydroxy-24-oxo-vitamin $D_3$ and 1,23,25-trihydroxy-24-oxo-vitamin $D_3$. Arch Biochem Biophys 224:671–676.

Molnár F, Sigüeiro R, Sato Y, Araujo C, Schuster I, Antony P, Peluso J, Muller C, Mouriño A, Moras D, Rochel N. 2011. 1α,25$(OH)_2$-3-epi-vitamin $D_3$, a natural physiological metabolite of vitamin $D_3$: Its synthesis, biological activity and crystal structure with its receptor. PLoS ONE 6:e18124.

Morrison NA, Eisman JA. 1991. Nonhypercalcemic 1,25-$(OH)_2D_3$ analogs potently induce the human osteocalcin gene promoter stably transfected into rat osteosarcoma cells (ROSCO-2). J Bone Miner Res 6:893–899.

Nagpal S, Na S, Rathnachalam R. 2005. Noncalcemic actions of vitamin D receptor ligands. Endocr Rev 26:662–687.

Nakagawa N, Sowa Y, Kurobe M, Ozono K, Siu-Caldera ML, Reddy GS, Uskokovic MR, Okano T. 2001. Differential activities of 1α,25-dihydroxy-16-ene-vitamin $D_3$ analogs and their 3-epimers on human promyelocytic leukemia (HL-60) cell differentiation and apoptosis. Steroids 66:327–337.

Norman AW, Bouillon R, Farach-Carson MC, Bishop JE, Zhou LX, Nemere I, Zhao J, Muralidharan KR, Okamura WH. 1993. Demonstration that 1β,25-dihydroxyvitamin $D_3$ is an antagonist of the nongenomic but not genomic biological responses and biological profile of the three A-ring diastereomers of 1α,25-dihydroxyvitamin $D_3$. J Biol Chem 268:20022–20030.

Omura T, Sato R. 1964. The carbon monoxide-binding pigment of liver microsomes. J Biol Chem 239:2379–2385.

Penning TM, Bennett MJ, Smith-Hoog S, Schlegel BP, Jez JM, Lewis M. 1997. Structure and function of 3α-hydroxysteroid dehydrogenase. Steroids 62:101–111.

Plum LA, DeLuca HF. 2010. Vitamin D, disease and therapeutic opportunities. Nat Rev Drug Discov 9:941–955.

Posner GH, Guyton KZ, Kensler TW, Barsony J, Lieberman ME. 1993. 1-(hydroxyalkyl)-25-hydroxyvitamin $D_3$ analogs of calcitriol. II: Preliminary biological evaluation Bioorg Med Chem Lett 3:1835–1840.

Rao DS, Campbell MJ, Koeffler HP, Ishizuka S, Uskokovic MR, Spagnuolo P, Reddy GS. 2001. Metabolism of 1α,25-dihydroxyvitamin $D_3$ in human promyelocytic leukemia (HL-60) cells: In vitro biological activities of the natural metabolites of 1α,25-dihydroxyvitamin $D_3$ produced in HL-60 cells. Steroids 66:423–431.

Reddy GS, Tserng KY. 1989. Calcitroic acid, end product of renal metabolism of 1,25-dihydroxyvitamin $D_3$ through the C-24 oxidation pathway. Biochemistry 28:1763–1769.

Reddy GS, Jones G, Kooh SW, Fraser D. 1982a. Inhibition of 25-hydroxyvitamin $D_3$-1-hydroxylase activity by chronic metabolic acidosis. Am J Physiol 243:E265–E271.

Reddy GS, Norman AW, Mayer E, Ho M, Tsang RC. 1982b. Study of 1,25-dihydroxyvitamin $D_3$ induced alterations in the metabolism of [$^3$H]25-hydroxyvitamin $D_3$ using isolated perfused kidneys from D-sufficient rats. Biochem Biophys Res Commun 107:922–928.

Reddy GS, Jones G, Kooh SW, Fraser D, DeLuca HF. 1983. Stimulation of 24,25 dihydroxyvitamin $D_3$ synthesis by metabolites of vitamin D. Am J Physiol 245: E359–E364.

Reddy GS, Tserng KY, Thomas BR, Dayal R, Norman AW. 1987. Isolation and identification of 1,23-dihydroxy-24,25,26,27-tetranorvitamin $D_3$, a new metabolite of 1,25-dihydroxyvitamin $D_3$ produced in rat kidney. Biochemistry 26:324–331.

Reddy GS, Clark JW, Tserng KY, Uskokovic MR, McLane JA. 1993. Metabolism of 1,25$(OH)_2$-16-ene-$D_3$ in kidney: Influence of structural modification of D-ring on side chain metabolism. Bioorg Med Chem Lett 3:1879–1884.

Reddy GS, Muralidharan KR, Okamura WH, Tserng KY, McLane JA. 1994. Metabolism of 1α,25-dihydroxyvitamin $D_3$ and one of its A-ring diastereomer 1α,25-dihydroxy-3-epi-vitamin $D_3$ in neonatal human keratinocyte. In: Norman AW, Bouillon R, Thomasset M, editors. Vitamin D, a pluripotent steroid hormone: Structural studies, molecular endocrinology and clinical applications. New York: Walter de Gruyter. pp 172–173.

Reddy GS, Siu-Caldera ML, Schuster I, Astecker N, Tserng KY, Muralidharan KR, Okamura WH, McLane JA, Uskokovic MR. 1997. Target tissue specific metabolism of 1α,25-dihydroxyvitamin $D_3$ through A-ring modification. In: Norman AW, Boullion R, Thomasset M, editors. Vitamin D—Chemistry, biology and clinical applications of the steroid hormone. Riverside: University of California. pp 139–146.

Reddy GS, Rao DS, Siu-Caldera ML. 2000. Natural metabolites of 1α,25-dihydroxyvitamin $D_3$ and its analogs. In: Norman AW, Boullion R, Thomasset M, editors. Vitamin D endocrine system: Structural, biological, genetic and clinical aspects. Riverside: University of California. pp 965–972.

Reddy GS, Muralidharan KR, Okamura WH, Tserng KY, McLane JA. 2001. Metabolism of 1α,25-dihydroxyvitamin $D_3$ and its C-3 epimer, 1α,25-dihydroxy-3-epi-vitamin $D_3$ in neonatal human keratinocytes. Steroids 66:441–450.

Reddy GS, Omdahl JL, Robinson M, Wang G, Palmore GTR, Vicchio D, Yergey AL, Tserng KY, Uskokovic MR. 2006. 23-Carboxy-24,25,26,27-tetranorvitamin $D_3$ (calcioic acid) and 24-carboxy-25,26,27-trinorvitamin $D_3$ (cholacalcioic acid): End products of 25-hydroxyvitamin $D_3$ metabolism in rat kidney through C-24 oxidation pathway. Arch Biochem Biophys 455:18–30.

Rehan VK, Torday JS, Peleg S, Gennaro L, Vouros P, Padbury J, Rao DS, Reddy GS. 2002. 1α,25-dihydroxy-3-epi-vitamin $D_3$, a natural metabolite of 1α,25-dihydroxyvitamin $D_3$: Production and biological activity studies in pulmonary alveolar type II cells. Mol Genet Metab 76:46–56.

Rhieu SY, Annalora AJ, Gathungu RM, Vouros P, Uskokovic MR, Schuster I, Palmore GTR, Reddy GS. 2011. A new insight into the role of rat cytochrome P450 24A1 in metabolism of selective analogs of 1α,25-dihydroxyvitamin $D_3$. Arch Biochem Biophys 509:33–43.

Rosen CJ, Adams JS, Bikle DD, Black DM, Demay MB, Manson JE, Murad MH, Kovacs CS. 2012. The nonskeletal effects of vitamin D: An endocrine society scientific statement. Endocr Rev 33:456–492.

Sagara Y, Wada A, Takata Y, Waterman MR, Sekimizu K, Horiuchi T. 1993. Direct expression of adrenodoxin reductase in *Escherichia coli* and the functional characterization. Biol Pharmacol Bull 16:627–630.

Sakaki T, Sawada N, Nonaka Y, Ohyama Y, Inouye K. 1999. Metabolic studies using recombinant *Escherichia coli* cells producing rat mitochondrial CY P24: CYP24 can convert 1α,25-dihydroxyvitamin $D_3$ to calcitroic acid. Eur J Biochem 262:43–48.

Sakaki T, Sawada N, Komai K, Shiozawa S, Yamada S, Yamamoto K, Ohyama Y, Inouye K. 2000. Dual metabolic pathway of 25-hydroxyvitamin D3 catalyzed by human CYP24. Eur J Biochem 267:6158–6165.

Sakurai R, Shin E, Fonseca S, Sakurai T, Litonjua AA, Weiss ST, Torday JS, Rehan VK. 2009. 1α,25$(OH)_2D_3$ and its 3-epimer promote rat lung alveolar epithelial-mesenchymal interactions and inhibit lipofibroblast apoptosis. Am J Physiol Lung Cell Mol Physiol 297:L496–L505.

Schuster I. 2011. Cytochrome P450 are essential players in the vitamin D signaling system. Biochim Biophys Acta 1814:186–199.

Schuster I, Astecker N, Egger H, Herzig G, Reddy GS, Schmid J, Vorisek G. 1997. Vitamin D metabolism in human keratinocytes and biological role of products. In: Norman AW, Boullion R, Thomasset M, editors. Vitamin D—Chemistry, biology and clinical applications of the steroid hormone. Riverside: University of California. pp 551–558.

Schuttelkopf AW, van Aalten DMF. 2004. PRODRG: A tool for high-throughput crystallography of protein-ligand complexes. Acta Crystallogr Sect D-Biol Crystallogr 60:1355–1363.

Sekimoto H, Siu-Caldera ML, Weiskopf A, Vouros P, Muralidharan KR, Okamura WH, Uskokovic MR, Reddy GS. 1999. 1α,25-Dihydroxy-3-epi-vitamin $D_3$: In vivo metabolite of 1α,25-dihydroxyvitamin $D_3$ in rats. FEBS Lett 448:278–282.

Shiohara M, Uskokovic M, Hisatake J, Hisatake Y, Koike K, Komiyama A, Koeffler HP. 2001. 24-Oxo metabolites of vitamin $D_3$ analogues: Disassociation of their prominent antileukemic effects from their lack of calcium modulation. Cancer Res 61:3361–3368.

Siu-Caldera ML, Clark JW, Santos-Moore A, Peleg S, Liu YY, Uskokovic MR, Sharma S, Reddy GS. 1996. 1α,25-Dihydroxy-24-oxo-16-ene vitamin $D_3$, a metabolite of a synthetic vitamin $D_3$ analog, 1α,25-dihydroxy-16-ene vitamin $D_3$, is equipotent to its parent in modulating growth and differentiation of human leukemic cells. J Steroid Biochem Mol Biol 59:405–412.

Siu-Caldera ML, Sekimoto H, Weiskopf A, Vouros P, Muralidharan KR, Okamura WH, Bishop J, Norman AW, Uskokovic MR, Schuster I, Reddy GS. 1999a. Production of 1α,25-dihydroxy-3-epi-vitamin $D_3$ in two rat osteosarcoma cell lines (UMR106 and ROS 17/2.8): Existence of the C-3 epimerization pathway in ROS 17/2.8 cells in which the C-24 oxidation pathway is not expressed. Bone 24:457–463.

Siu-Caldera ML, Sekimoto H, Peleg S, Nguyen C, Kissmeyer AM, Binderup L, Weiskopf A, Vouros P, Uskokovic MR, Reddy GS. 1999b. Enhanced biological activity of 1α,25-dihydroxy-20-epi-vitamin $D_3$, the C-20 epimer of 1α,25-dihydroxyvitamin $D_3$, is in part due to its metabolism into stable intermediary metabolites with significant biological activity. J Steroid Biochem Mol Biol 71:111–121.

Swami S, Zhao XY, Sarabia S, Siu-Caldera ML, Uskokovic M, Reddy GS, Feldman D. 2003. A low-calcemic vitamin D analog (Ro 25-4020) inhibits the growth of LNCaP human prostate cancer cells with increased potency by producing an active 24-oxo metabolite (Ro 29-9970). Recent Results Cancer Res 164:349–352.

Uskokovic MR, Manchand P, Marczak S, Maehr H, Jankowski P, Adorini L, Reddy GS. 2006. C-20 cyclopropyl vitamin $D_3$ analogs. Curr Top Med Chem 6:1289–1296.

Verstuyf A, Carmeliet G, Bouillon R, Mathieu C. 2010. Vitamin D: A pleiotropic hormone. Kidney Int 78:140–145.